Two-Dimensional Zeeman Polarization Spectroscopy of Tunneling Atomic Groups in Solids

J. Peternelj,[1] A. Damyanovich,[2] and M. M. Pintar[3]
[1]*Faculty of Civil and Geodetic Engineering, University of Ljubljana, Ljubljana, Slovenia, and J. Stefan Institute, Ljubljana, Slovenia*
[2]*Department of Medical Imaging, University of Toronto, Toronto, Ontario*
[3]*Department of Physics, University of Waterloo, Waterloo, Ontario N2L 3G1*
(Received 9 September 1998)

A spectral line at the rotational tunneling frequency ω_T, due to nonmagnetic transitions within the ground state manifold of a tunneling atomic group, has been observed in the Fourier spectrum of Zeeman polarization evolution in the rotating frame of proton spins. These observations suggest a new 2D NMR method. We propose that the underlying conditions which make the nonmagnetic ω_T peak observable in NMR experiments are quite general and are related to the properties of dipolar interaction under spin rotations. [S0031-9007(99)08732-3]

PACS numbers: 76.60.–k, 33.25.+k, 73.40.Gk

In a series of field cycling experiments, Horsewill *et al.* [1,2] observed a spectral line at the rotational tunneling frequency [3] ω_T, which was interpreted as being due to nonmagnetic transitions within the ground state manifold of a tunneling methyl group. We want to show that this observation is not specific for field cycling experiments nor for methyl groups, and that, in general, the nonmagnetic transitions affect the time evolution of nuclear Zeeman polarization.

NMR spectroscopic information about the dynamics of an atomic group containing protons is obtained by measuring its Zeeman polarization:

$$\vec{M}(t) = \gamma_p \hbar \, \mathrm{Tr}\{\rho(t)\vec{I}\}, \tag{1}$$

where γ_p is the proton magnetogyric factor, $\vec{I}$ is the total proton spin, and $\rho(t)$ is the density matrix whose time evolution is governed by the Hamiltonian $H = H_Z + H_R + H_D + H_{\mathrm{rf}}(t)$. The meaning of the various terms is as follows: $H_Z = -\hbar\omega_0 I_z$ is the Zeeman Hamiltonian, H_R is the rotational Hamiltonian [4], H_D is the dipole-dipole interaction term [5], and the rf Hamiltonian is $H_{\mathrm{rf}}(t) = -\gamma_p \hbar \vec{I} \cdot \vec{H}_{\mathrm{rf}}(t)$. The proton Larmor frequency in the static magnetic field $\vec{H}_0$, whose direction defines the z axis of the laboratory fixed coordinate system, is $\omega_0 = \gamma_p H_0$. The radio-frequency pulse employed to make the coupling between the rotational motion and spin dynamics experimentally observable ($\omega_0 \gg \omega_T$) is $\vec{H}_{\mathrm{rf}}(t)$. A representative Zeeman rotational energy level scheme is shown in Fig. 1.

Considering the form of the dipole-dipole interaction term [5] H_D, it follows that the transitions contributing to the Fourier spectrum of (1) are those associated with the change of the magnetic quantum number of the protons by $\Delta M = 0, \pm 1, \pm 2$. However, the relative magnitudes of the various energy terms are such that only the lines corresponding to $|\Delta M| = 1$ and 2 are observed normally, providing that the magnetization is measured immediately after the rf field is switched off. In actual experiments, however, there is, due to dead time, always a time delay τ between the end of the field pulse and the instant when the magnetization is measured. Therefore, to be rigorous, the time evolution of the magnetization during this time interval should be accounted for also. When this is done, the Fourier transform of the magnetization $\vec{M}(t + \tau)$ with respect to time t (t denotes the duration of the rf field pulse) shows the $\Delta M = 0$ line, the so-called ω_T peak, of observable intensity.

As a specific example, let us consider a tunneling methyl group in a static field $\vec{H}_0$ and rotating transverse rf field at exact resonance. In this case, referred to as normal rotating frame, we have $H_{\mathrm{rf}}(t) = -\hbar\omega_1[I_x \cos\omega_0 t - I_y \sin\omega_0 t]$, where $\omega_1 = \gamma_p H_1$, and H_1 is the magnitude of the rotating rf field. Measuring the x component of the magnetization $M_x(t + \tau)$, and retaining only the

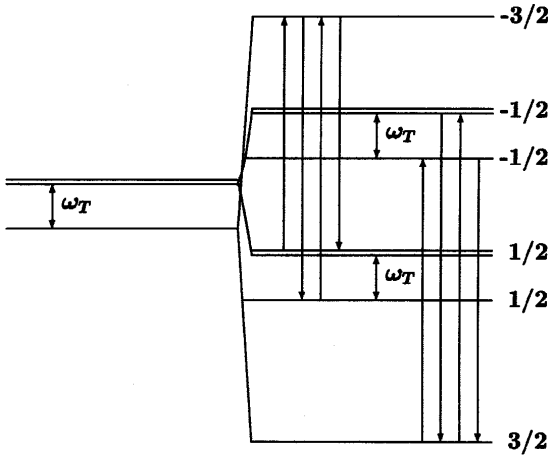

FIG. 1. Schematic reproduction of the energy level scheme for an isolated tunneling methyl group. The arrows indicate the matrix elements of dipolar Hamiltonian contributing to $\Delta M = 0$ transitions. The numbers on the right represent the z component of the CH_3-proton spin corresponding to the given eigenstate of Zeeman Hamiltonian.

$\Delta M = 0$ terms which are due solely to the time evolution during the time delay τ, we obtain

$$M_x(t + \tau; \Delta M = 0)/\gamma_p \hbar = \{A(\beta, \tau)[1 + \cos \Omega(\beta) t] - B(\beta, \tau)\} \cos \omega_0 (t + \tau), \quad (2)$$

where we have defined

$$A(\beta, \tau) = F(\beta)\{1 + \cos \Omega(\beta)\tau - 2\cos[\Omega(\beta)\tau/2] \times \cos \omega(\beta)\tau\}, \quad (3)$$

$$B(\beta, \tau) = F(\beta)\{\sin \Omega(\beta)\tau - 2\sin[\Omega(\beta)\tau/2] \times \cos \omega(\beta)\tau\} \sin \Omega(\beta)\tau, \quad (4)$$

$$\omega(\beta) = \frac{1}{2}\omega_T - \frac{9}{32}\omega_D(1 - 3\cos^2 \beta), \quad (5)$$

and

$$\Omega(\beta) = \left\{\left[\omega_T + \frac{3}{16}\omega_D(1 - 3\cos^2 \beta)\right]^2 + \frac{81}{128}\omega_D^2 \sin^4 \beta\right\}^{1/2}. \quad (6)$$

In the above equations, $\omega_D = \gamma_p^2 \hbar / R_0^3$ is the dipolar frequency (where $R_0 = 1.78$ Å is the CH_3 proton-proton distance), and β is the angle between the methyl group symmetry axis and the direction of the external magnetic field $\vec{H}_0$. The function $F(\beta)$ is rather lengthy and will not be given since it is not needed for the discussion that follows (it will be used, however, to plot Fig. 2).

The $\Delta M = 0$ contribution to $M_x(t + \tau)$ is due to time evolution of the spin-rotational system during time interval τ, governed by $H_Z + H_R + H_D$ and, as seen from (3) and (4), vanishes in the $\tau \to 0$ limit. It follows from (2) that, in spite of $\omega_0 \gg \omega_T, \omega_D$, the dipolar interaction does affect spin dynamics in the high field through its secular part modulated by tunneling motion. This comes about because the secular dipolar interaction in the high field acquires in the rotating frame additional terms [5] which generate $\Delta M = \pm 2$ transitions responsible for the ω_T peak (Fig. 1). In the case when $\omega_1 \gg \omega_D$, the intensity of this peak is proportional to $\omega_D^2/[(2\omega_1)^2 - \omega_T^2]$, and is thus comparable to the intensity $\omega_D^2/(2\omega_1 - \omega_T)^2$ of the tunneling satellite centered at $2\omega_1 - \omega_T$. Their ratio for methylmalonic acid, a well studied material with a CH_3 tunneling splitting of $\approx$71 kHz, is approximately 1 at $H_1 = 25$ G.

The Fourier transform of (2), with respect to t, is defined as

$$M_x(\omega, \tau) = \frac{1}{\sqrt{2\pi}} \int_{-\infty}^{\infty} dt\, e^{i\omega(t+\tau)} M_x(t + \tau). \quad (7)$$

For a given orientation of the methyl group with respect to the direction of the external magnetic field $\vec{H}_0$, the Fourier components contributing to the $\Delta M = 0$ line of (7) are centered at $\omega = \Omega(\beta)$ as defined by (6). To compare the calculations with the experiments which were done on powdered polycrystalline samples, we have to average (7) with respect to β. By broadening the calculated spectra with a Gaussian function with a broadening parameter σ, and taking the absolute value of the real part of (7), the spectrum shown in Fig. 2 is obtained. Please note that, instead of ω, the off-field $H = (\omega - \omega_0)/\gamma_p$ is used as

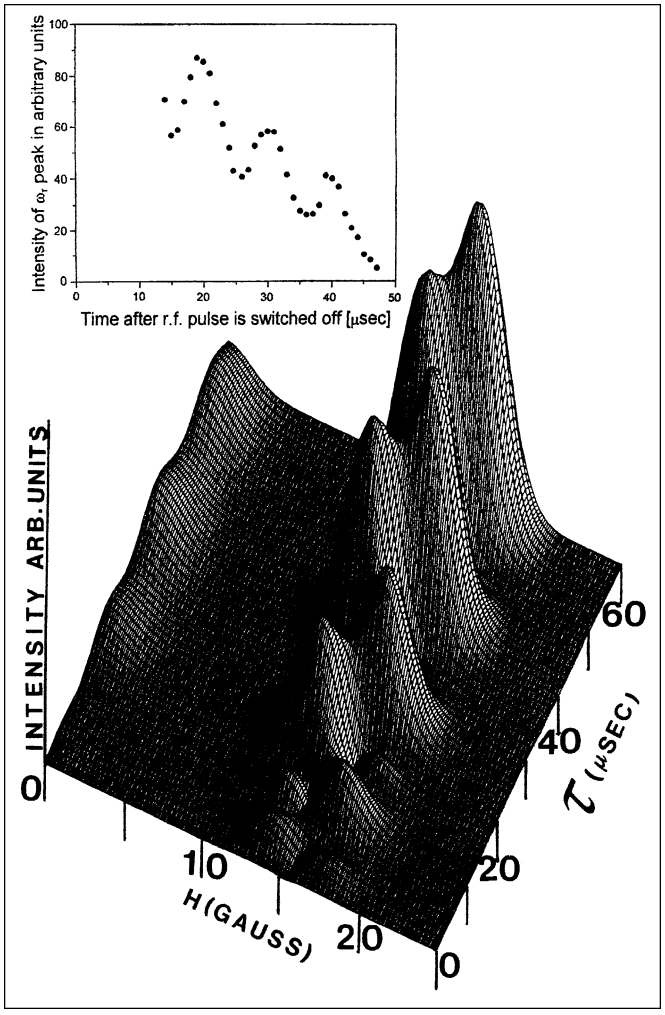

FIG. 2. The calculated spectrum of the magnetization evolution of a CH_3 group in the rotating frame, shown as a function of time delay τ, after the rf field pulse has been switched off. The selected tunneling frequency is $\omega_T/\gamma_P = 15$ G, $\omega_1/\gamma_P = 45$ G, and the broadening parameter $\sigma = 1$ G. Note that the position of the nonmagnetic ($\Delta M = 0$) peak depends on τ as well. It should be kept in mind, however, that the growth of the $\Delta M = 0$ peak intensity is eventually attenuated because of the T_2-type spin dephasing. This consequence of the dipole-dipole interaction was not taken into account in this calculation. Since T_2 of the CH_3 group is around 20 μsec and even shorter for the NH_4 group, the tunneling peak decays to noise level in about 50 μsec. In the inset, the oscillations of the $\Delta M = 0$ spectral line intensity (in the magic tilt experiment) in NH_4I are shown. In this case, the intensity of the ω_T peak oscillates while the position of the peak does not. The main tunneling splitting in this material is 77 kHz. The period of the oscillations shown in the inset is approximately 11 μsec, which corresponds to a frequency of $\approx$90 kHz.

a variable. We notice that the intensity and the position of the $\Delta M = 0$ peak depend on the time delay τ (see Fig. 2). For example, for $\tau > 15$ μsec, the intensity of the real part of the powder average $\langle M_x(H, \tau; \Delta M = 0)\rangle$ becomes comparable and often larger than the intensity of the low-field tunneling satellite centered at $2H_1 - \omega_T/\gamma_p$. Unfortunately, the dead time of the NMR spectrometer limits the experimentally accessible range of τ values to the (10–30) μsec interval. The imaginary part of $\langle M_x(H, \tau; \Delta M = 0)\rangle$ is not shown in Fig. 2 because it is qualitatively similar to the real part.

These predictions were confirmed by experiments [6] performed on CH_3CD_2I ($\omega_T/\gamma_p \cong 4.3$ G) and methylmalonic acid ($\omega_T/\gamma_p \cong 17$ G). Measurements of the proton magnetization in the rotating frame were made using the spin-locking pulse sequence $A[\pi/2]_y - B[H_1(t)]_x$. The pulse A of this sequence rotates the equilibrium magnetization through 90° into the x-y plane, where it is "locked" along the rf field pulse B. This prepares the initial state of the system, $\rho(t = 0)$. The subsequent evolution of the spin system during the time interval t, when the field pulse $\vec{H}_{\rm rf}(t)$ is on, and during the time interval τ in the main magnetic field (after the field pulse has been switched off), is monitored by detecting the amplitude of the decaying transverse magnetization. By increasing the length of the rf pulse in unit increments $\Delta t = 1$ μsec, for a total of $N \cong 200$ progressively longer spin-locking times (each pulse group is delayed from its predecessor long enough to allow for a spin-rotational system to reach thermal equilibrium with the lattice), we obtain a quasicontinuous oscillatory pattern which by Fourier transform yields the spectrum. Furthermore, the real (absorption) and imaginary (dispersion) components of the magnetization are acquired separately using quadrature detection at 40 or more different τ values, or "time windows," along the free induction decay. Because of receiver dead time ($\approx$10 μsec), the first time window is delayed by 12 μsec following the end of the rf field pulse, with subsequent time windows progressively delayed by an additional 1.4 μsec each. Thus, a magnetization array (40×200) of $\langle M_x(t + \tau)\rangle$ was obtained as a function of both, the rf pulse duration t and the detection window time τ, for each detector channel. For each solid, the 90-degree pulse A was 50 G (of 1.2 μsec duration) and the rf field pulse B amplitude H_1 chosen in such a way that the ω_T peak and the low-field tunneling satellite at $\omega_1 - \omega_T$, did not overlap.

To improve the resolution of the $\Delta M = 0$ tunneling line and satellites, the magnetization was also measured in the rotating frame tilted [7] at the magic angle, $\Theta_M = 54°$, with respect to the external magnetic field $\vec{H}_0$ using the same experimental acquisition method described above. In this frame, the secular part of the dipolar interaction vanishes, resulting in narrower spectral peaks ($\approx$3 kHz) and, in addition, the dipolar shifts of the spectral lines become negligible.

In general, in all of the spectra, the nonmagnetic peak at ω_T, as well as the main dipolar peaks at $2\omega_1$ and ω_1 with their tunneling satellites at $2\omega_1 \pm \omega_T$ and $\omega_1 \pm \omega_T$, are observed. The up-field satellites $2\omega_1 + \omega_T$ and $\omega_1 + \omega_T$, however, are often lost in noise. The inset in Fig. 2 shows the oscillations of the $\Delta M = 0$ peak amplitude in NH_4I, acquired in magic frame at 30 K, at proton frequency 30 MHz, as a function of τ. In this material, the oscillatory dependence of the peak intensity on τ is clearly visible. The Fourier transform of this pattern yields a frequency which is about 15% larger than its ω_T of $2\pi \times 77$ kHz (see Fig. 2). This difference is due to the remaining small dipolar shifts as seen from (6).

In conclusion, the reported observation of the $\Delta M = 0$ peak of a tunneling atomic group by Horsewill *et al.* [1,2] has been complemented by measuring the time evolution of the magnetization in the rotating frame. The analysis described above has shown that, in order to make this line observable in NMR experiments, it is essential that nuclear spins are subjected to a sequential time evolution governed by two distinct Hamiltonians defined on the time intervals $(0, t)$ and $(t, t + \tau)$, respectively. Since this method offers the possibility of two-dimensional Fourier analysis (with respect to t and τ) of the experimental data, it could be termed the two-dimensional Zeeman polarization spectroscopy. This technique will delineate the tunneling peaks better, particularly in those systems exhibiting multiple tunneling frequencies.

The $\Delta M = 0$ mechanism described applies to the experiments done by Horsewill *et al.* [1,2]. However, these conclusions are quite general and should apply in all cases of rotational tunneling of atomic groups in solids, as well as in other spectroscopic methods where sequential evolutions can be monitored experimentally.

This research was supported by the Canadian National Science and Engineering Research Council.

[1] A. J. Horsewill and A. Aibout, J. Phys. Condens. Matter **1**, 10 533 (1989).
[2] M. J. Barlow, S. Clough, P. A. Debenham, and A. J. Horsewill, J. Phys. Condens. Matter **4**, 4165 (1992).
[3] J. Peternelj and T. Kranjc, Z. Phys. B **92**, 61 (1993).
[4] J. Peternelj, T. Kranjc, and M. M. Pintar, Phys. Rev. B **54**, 955 (1996).
[5] P. S. Hubbard, Rev. Mod. Phys. **33**, 249 (1961).
[6] A. Damyanovich, J. Peternelj, and M. M. Pintar, Physica (Amsterdam) **202B**, 273 (1994).
[7] C. P. Slichter, *Principles of Magnetic Resonance* (Springer-Verlag, Berlin, 1990), 3rd ed.